PHYSICAL REVIEW B VOLUME 36, NUMBER 6 15 AUGUST 1987-II

# Order and disorder in iron-titanium

E. Z. da Silva
*Instituto de Física Gleb Wataghin, Universidade Estadual de Campinas, Caixa Postal 6165, Campinas 13 081, São Paulo, Brazil*

P. Strange
*Department of Physics, University of Bristol, Tyndall Avenue, Bristol BS8 1TL, United Kingdom*

W. M. Temmerman
*Daresbury Laboratory, United Kingdom Science and Engineering Research Council, Daresbury, Warrington WA4 4AD, United Kingdom*

B. L. Gyorffy
*Department of Physics, University of Bristol, Tyndall Avenue, Bristol BS8 1TL, United Kingdom*

(Received 17 March 1987)

We have studied the electronic structure of the ordered intermetallic compound Ti-Fe with CsCl structure and a corresponding hypothetical random solid solution on a bcc and CsCl lattice using comparable first-principles self-consistent calculations. The differences of the one-electron spectra enable us to comment on the nature of bonding and the absence of disorder in this interesting system.

## I. INTRODUCTION

The nature of the metallic bonding has always been a central issue in solid-state physics.[1] Over the past two decades the main contributions to this subject have come from first-principles calculations of cohesive energies, (1–5 eV) bulk moduli, and equilibrium lattice parameters of pure metals and ordered metallic compounds.[2] To a large measure these advances have been made possible by the rapidly improving computational techniques for implementing the local-density approximation to the density-functional description of the inhomogeneous electron liquid.[3] Recently, these have reached a level of sophistication where the yet deeper question of structural energies ($\sim 0.1$ eV), namely the differences between the ground-state energies of the same metal with different crystal structures, can be raised.[4] Here we wish to capitalize on current progress in calculating the electronic structure of disordered systems[5] and consider the similarly difficult problem of the ordering energies (0.1 eV) which determine the compositional structure of binary alloys and drive the order-disorder transformations.[6]

Of course, the role of electrons in clustering and ordering of the constituents in metallic alloys has been recognized for a long time.[7] However, the consideration of the relevant factors: size effect, electronegativity, and electron per atom ratio, $e/a$, on equal footing and on the basis of first-principles calculations has become a possibility only with the advent of the self-consistent-field Korringa-Kohn-Rostoker coherent-potential-approximation SCF-KKR-CPA band-theory method for random alloys.[8,9] Although no total-energy calculations using the SCF-KKR-CPA have been reported as yet, it has been demonstrated that one-electron spectra can be calculated reliably by this method even in alloys with charge transfer.[3] Making use of this advance, and as a preliminary to calculating actual energy differences between ordered and disordered phases, we present here the first *ab initio* comparative study of the corresponding electronic structures. Our aim is to illustrate that even such a limited, but by no means simple, exercise can lead, under favorable circumstances, to valuable insights concerning the electronic origin of ordering and throw light on the connection between bonding and compositional long- and short-range order. As an extreme example of strongly ordering alloys we chose to study the Ti-Fe system.

One of the most common ordered binary-alloy crystal structures is that of cesium chloride (CsCl). As many as 160 alloys form this structure.[10] A graph of abundance of these intermetallic compounds against $e/a$ shows two peaks. The first is around $e/a=\frac{3}{2}$ which corresponds to CuZn for instance. The other is at $e/a=6$ where we find Ti-Fe. In general, this peak is the result of two tendencies: one is the preference of alloys, with $e/a=6$ and stoichiometric composition to form bcc solid solutions on crystallization[11] and the other is to order with the CsCl structure.[12] In the case of Ti-Fe the ordering tendency is so strong that there is no disordered phase below the melting temperature and it is only for Ti-rich Ti-Fe alloys with $c>77\%$ that the phase diagram[10] indicates a continuous, high temperature ($T>1085$ K) phase field of bcc random solid solution up to pure Ti.

Since the atomic radius of Ti is some 15% larger than that of Fe one might suppose that the order is due to the size effect, i.e., the natural propensity of the large and small spheres to pack in a regular fashion. However, the Wigner-Seitz radius of Ti-Fe is a spectacular 4% lower than would be predicted by Vegard's law. Such contraction is usually taken to be evidence for strong bonds. Indeed, by this measure Ti—Fe exhibits the strongest interatomic bond among metals. Thus, in simple chemical language one could say that Ti-Fe ordering occurs to satisfy all the strong Ti—Fe bonds.

While this is an attractive argument it cannot be literally true since the cohesive energy of a metal cannot be attributed to pairwise bonds in general. Nevertheless, it is of considerable interest to investigate the extent to which this simple picture can be recaptured in terms of electronic energy bands appropriate to the description of infinite solids. The primary aim of our calculations is to do just that.

Before proceeding to our discussion of how this might be achieved we wish to pause to note that besides a good example of strongly ordering alloys, Ti-Fe is an interesting metal in its own right. It is exceptionally hard and, from the point of view of technological applications unfortunately, it is very brittle. However, this shortcoming can be overcome by various additives and it is the base of many steels. Moreover it is a very good hydrogen absorber and as such it is a promising material in the technology of hydrogen storage. We hope that a deeper understanding of the forces which bind it together might be helpful in these applications.

Returning to our main theme we note that a specific band theoretic mechanism which leads to ordering in binary alloys has been described in detail by Gyorffy and Stocks.[13] They have shown that parallel sheets of well-defined Fermi surfaces can exist in random alloys and, furthermore, they can give rise to incommensurate modulations of the concentration with wave vectors equal to the spanning vectors. This effect is believed to be at work in many fcc alloys, such as $Cu_3Pd$ and $Cu_3Au$, which form long-period structures. In Ti-Fe and other alloys based on the bcc structure another mechanism appears to govern the tendency towards order. It does not involve the shape of the Fermi surface directly and, as we shall show, it relies on lowering the energy of the one-electron energy bands quite some distance from the Fermi energy.

To see how the above mechanism might operate consider an alloy of an early (Ti) and a late (Fe) transition metal with concentration so that $e/a=6$. Assume that there is one electron per atom in the $s$ band and that the rigid-band model is applicable.[14] Then note that a generic feature of $d$ bands on a bcc lattice is that they split, almost symmetrically about the energy of the atomic $d$ state, into two well-defined, bonding and antibonding groups of states separated by a deep minimum in the density of states. Thus when such bands are half-filled the cohesive energy is particularly high and the lattice parameter is particularly small as in the middle of the transition-metal series.[15] For 5 $d$ electrons our rigid $d$ bands are half-filled and hence the above mechanism could explain, at least qualitatively, the preference of our alloys for the bcc structure and the lattice contraction in Ti-Fe.

However, this argument can say nothing about ordering because in the rigid-band model the conduction electrons do not differentiate between sites which are occupied by different species of atoms. Evidently to explain the preference for CsCl order within framework we must have the bonding states at lower energies in the ordered state than in the disordered state. To show that this is indeed the case we have calculated the energy bands in both phases (Table I).

To be comparable both calculations are based on the same first-principles description of the crystal potentials. The strong ordering tendency in Ti-Fe suggests that an electron "sees" a very different potential well on the Ti sites than on the Fe sites. Therefore in the disordered state we have made use of the coherent-potential approximation (CPA) which, in contrast to the rigid-band model, is known to describe alloys with very different constituents.[16,17,18]

The calculations outlined above could have been usefully performed on the basis of simple model Hamiltonians and thereby much effort would have been solved. However, such models become unreliable once substantial charge transfer has to be allowed for. Unfortunately, this is precisely the case in the problem at hand.

Because the rigid-band model overlooks the difference between the species and therefore distributes the $e/a$ electrons per atom uniformly among the unit cells, it gives rise to a very significant amount of charge transfer. More generally, if an alloy of early and late transition metals is to benefit energetically from filling only the bonding half of its $d$ band some of the filled antibonding states of the late transition metal must be emptied into the unfilled $d$ band of the species from the beginning of the transition-metal series. This rearrangement of states in turn will give rise to charge rearrangements and in order to take this properly into account all our calculations are fully self-consistent with respect to charge, in the spirit of the density-functional theory. Clearly without a serious consideration of the charge rearrangements on alloying, the qualitative conclusions become even impossible for these systems.

One might also have been tempted to address the problem of bonding in Ti-Fe by comparing self-consistent calculations for the ordered intermetallic compound Ti-Fe and for the corresponding pure metals. However, because of the large charge rearrangements mentioned above few definitive conclusions could be expected to emerge from such work. Thus only the large scale, fully self-consistent, comparative study of the ordered and disordered phases we have undertaken appears to have a chance of shedding light on the questions we have raised.

The general outline of our method of presentation should be clear from the section headings.

## II. DESCRIPTION OF THE CALCULATIONS

In order to understand why there is no disordered phase observed in TiFe we have performed electronic structure calculations in both the ordered and disordered cases.

The ordered phase of TiFe was examined using the linear muffin-tin-orbital method of Andersen[19,20] and local-density-functional theory. The observed crystal structure of TiFe is the well-known cesium chloride structure. Spin-orbit coupling was neglected in the calculation, but all other relativistic corrections were included. Within this method the relative size of the spheres around each ion is an arbitrary quantity. However, to facilitate comparison with the disordered case we have chosen the sphere sizes equal. To achieve self-

TABLE I. Comparison of the ordered and the disordered states at the higher symmetry points of the CsCl Brillouin zone.

| Ordered | | Disordered | | Ordered | | Disordered | | Ordered | | Disordered | | Ordered | | Disordered | |
|---|---|---|---|---|---|---|---|---|---|---|---|---|---|---|---|
| $\Gamma_1$ | 0.191 | 0.200 | $\Gamma_1$ | $R_{15}$ | 0.591 | | | $X_4$ | 0.453 | | | $M_1$ | 0.428 | | |
| | | | | | | 0.586 | $R_{15} \equiv R_{25'}$ | | | 0.462 | $X_1 \equiv X_4$ | | | 0.449 | $M_1 \equiv M_3$ |
| $\Gamma_{12}$ | 0.462 | 0.462 | $\Gamma_{12}$ | $R_{25'}$ | 0.603 | | | $X_1$ | 0.474 | | | $M_3$ | 0.477 | | |
| $\Gamma_{25'}$ | 0.674 | 0.699 | $\Gamma_{25'}$ | $R_{12'}$ | 0.747 | 0.748 | $(R_{12} \equiv R_{12'})^1$ | | | | | $M_5$ | 0.592 | 0.586 | $M_5$ |
| | | | | | | | | $X_{3'}$ | 0.593 | | | | | | |
| | | 0.736 | $\Gamma_{12}^{u,1}$ | $R_{12}$ | 0.989 | 0.986 | $(R_{12} \equiv R_{12'})^2$ | | | 0.624 | $X_2 \equiv X_{3'}$ | $M_4$ | 0.744 | 0.749 | $(M_2 \equiv M_4)^1$ |
| $\Gamma_{12}^{u}$ | 0.830 | | | | | | | $X_2$ | 0.699 | | | | | | |
| | | 0.973 | $\Gamma_{12}^{u,2}$ | | | | | | | | | $M_3$ | 0.749 | | |
| | | | | | | | | $X_{5'}$ | 0.672 | 0.711 | $X_{5'} \equiv X_5$ | | | very smeared | $M_1 \equiv M_3$ |
| $\Gamma_{25}^{u'}$ | 0.971 | 1.011 | $\Gamma_{25}^{u'}$ | | | | | | | | | $M_1$ | 0.863 | | |
| | | | | | | | | $X_{2'}$ | 0.716 | | | | | | |
| | | | | | | | | | | very smeared | $X_{2'} \equiv X_3$ | $M_{5'}$ | 0.825 | 0.823 | $M_{5'}$ |
| | | | | | | | | $X_3$ | 0.926 | | | | | | |
| | | | | | | | | | | | | $M_2$ | 0.983 | 0.986 | $(M_2 \equiv M_4)^2$ |
| | | | | | | | | $X_5$ | 0.814 | very smeared | $X_{5'} \equiv X_5$ | | | | |
| | | | | | | | | | | | | $M_5$ | 0.968 | 1.035 | $M_5$ |
| | | | | | | | | $X_{4'}$ | 0.805 | 0.786 | $(X_1 \equiv X_{4'})^1$ | | | | |
| | | | | | | | | $X_1$ | 1.052 | 1.011 | $(X_1 \equiv X_{4'})^2$ | | | | |
| | | | | | | | | Fermi energy | | | | | | | |
| | | | | | | | | Ordered | Disordered | | | | | | |
| | | | | | | | | 0.747 | 0.732 | | | | | | |

consistency and calculate the density of states, 364 **k** points in the irreducible wedge of the Brillouin zone were used. All the results shown were obtained using the Hedin-Lundqvist approximation for the exchange-correlation energy. This calculation was also run with and without the LMTO combined correction terms.[19] These make an allowance for the difference between the atomic sphere and the real atomic polyhedron in the crystal. It was found in particular that the Fermi surface was extremely sensitive to this refinement and all the results shown include the combined correction term.

The hypothetical disordered phase of TiFe would be a bcc substitutionally disordered alloy $\mathrm{Ti}_{0.50}\mathrm{Fe}_{0.50}$. (In the present paper no short-range order is included). For this phase we have performed self-consistent-field KKR-CPA calculations.[5,16] Similar calculations for three other concentrations of Ti-rich TiFe alloys were performed. These will be reported elsewhere. Following Stocks and Win- ter,[5] we have first achieved self-consistency within the framework of a cluster CPA calculation with five atomic shells, and for the converged potential we did a full KKR-CPA (Ref. 21) as a final check.

Although titanium and iron have very different sizes and numbers of valence electrons we have used equal-sized spheres for each constituent in both calculations. This makes any statement about the absolute total charge transferred ambiguous. We do not attempt to resolve such ambiguities but concentrate on the changes of the charge redistribution on ordering. The changes in the charge transfer we find are genuine reflections for the charge flow in the system as the number of unlike neighbors increases with ordering.

## III. DISCUSSION OF THE RESULTS

Figure 1 shows the energy bands of the ordered intermetallic compound Ti-Fe along various symmetry directions of the Brillouin zone corresponding to the CsCl structure. These results are in good quantitative agreement with the previous calculations of Yamashida and Asano[22] and Papaconstantopoulos.[23] The lowest-lying band is an *s* band and, as expected, the Fermi energy falls right in the middle of a manifold of flat *d* bands and splits up the *d*-band complex. There are very few states crossing the Fermi energy. In particular, there is a band gap in the ⟨111⟩ direction. The Fermi surface is surprisingly small for a metal and consists of an electron pocket around the *X* point and an equal-sized hole pocket around the *M* point.[24]

A better view of the overall band structure is given by the density of states. This $n_t(E)$, and its components on Ti and Fe sites, $n_{\mathrm{Ti}}(E)$ and $n_{\mathrm{Fe}}(E)$, respectively, are shown in Fig. 2. Evidently, the *d*-band complex breaks into the two groups separated by a deep minima where the Fermi energy, $E_F$, falls. The lower states are predominantly Fe *d* states while those above the minima are mostly Ti *d* states. Interestingly, almost all structure in $n_{\mathrm{Fe}}(E)$ is repeated in $n_{\mathrm{Ti}}(E)$. This implies that states occur on both kinds of sites. Consequently, we may interpret the group of states below the minimum as Fe—Ti bonding states while those above are the corresponding antibonding states. Since only the bonding states are filled this situation appears to be an energetically very favorable one as we have envisioned it in the Introduction.

We will now investigate how the arrangement of states changes with the change in the state of order. The configurationally averaged total $\bar{n}_t(E)$ density of states in the disordered state is shown in Fig. 3. The partially averaged densities of states $\bar{n}_{\mathrm{Ti}}(E)$ and $\bar{n}_{\mathrm{Fe}}(E)$ on the Ti and Fe sites, respectively, are also displayed. The marked broadening of all structure is a clear sign of strong disordered scattering. The most conspicuous effect of this is that the "gap" at $E_F$ has practically disappeared. This suggests that many filled (unfilled) bands have been raised lowered) in energy and hence the total energy has in-

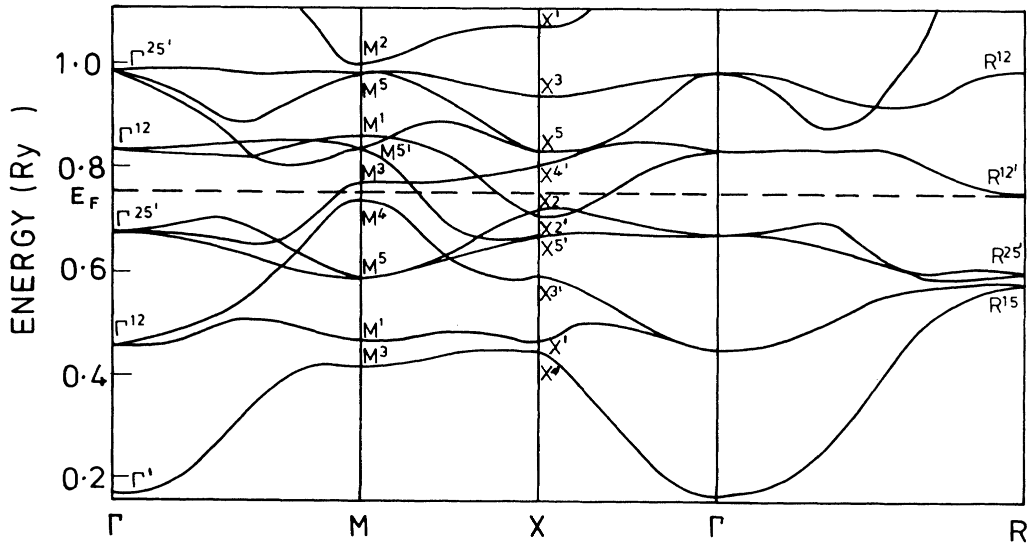

FIG. 1. The energy bands of ordered TiFe along several symmetry directions.

creased. Further evidence for this will be presented later when we examine the movement of the individual bands in detail.

A striking feature of the above results is the behavior of $\bar{n}_{\mathrm{Fe}}(E)$ and $\bar{n}_{\mathrm{Ti}}(E)$. Below $E=-0.15$ Ry they follow each other as did $n_{\mathrm{Fe}}(E)$ and $n_{\mathrm{Ti}}(E)$ in the ordered calculation. However, above $E=-0.15$ Ry they display a different structure: the maxima and the minima in the partial density of states do not follow each other any more as they did for the ordered calculation. This is characteristic behavior for alloy bands in the split-band regime.[16] It implies that states at a given energy are localized on one kind of site. For instance, the very numerous states near and just above $E_F$ in Fig. 3 have large amplitudes on the Fe sites but small amplitudes on the Ti sites. This is in contrast to a Ti-Fe bonding state where we would have a large amplitude on both the Ti and the Fe site.

To interpret the above phenomenon it is important to note that below $E=-0.15$ Ry the bonds are there roughly to the same extent as in the ordered state even though the number of unlike neighbors is much smaller in the disordered state. Moreover, the relative positions of their bonding states with respect to the Fermi energy have not been changed by the disorder. Thus Ti—Fe bonding, in the above sense, can occur without predominance of Ti-Fe nearest-neighbor pairs. On the other hand Ti—Fe bonding states seem to have disappeared in the energy range $-0.15\ \mathrm{Ry}<E<E_F$ in spite of the fact that there are quite a few Ti-Fe nearest-neighbor pairs even in the disordered state. These states have been replaced by states with large amplitudes either only on the Ti sites or only on the Fe states. These split-band states of the disordered phase come from the bonding (antibonding) states of the ordered system and occur therefore at higher (lower) energies. We will find that $E_F$ has not moved very much with respect to the atomic zero and therefore the above increase of energy could be the potential barrier which cannot be overcome by the entropic contribution to the free energy below the melting temperature. Namely, the stability of the ordered phase is due to this energy cost of disordering.

Before continuing our analysis of the above interesting hints as to the origin of order we wish to pause here to examine the bands involved in more detail.

In the disordered state the wave vector $\mathbf{k}$ is not a good quantum number. Thus, the nearest one can get to a band-by-band account of the electronic structure is a study of the Bloch spectral function $\bar{A}_B(\mathbf{k},E)$.[25] This may be regarded as the density of states at a point $\mathbf{k}$ in the Brillouin zone. Its integral over the Brillouin zone $\int_{\mathrm{BZ}} d^3k\, \bar{A}_B(\mathbf{k},E)$ is the total averaged density of states $\bar{n}_t(E)$. For an ordered system it consists of a set of $\delta$-functions peaks $A_B(\mathbf{k},E)=\sum_\nu \delta(E-E_{k,\nu})$ where $E_{k,\nu}$ is the Bloch energy eigenvalues for the $\nu$th band. For random solid solutions these peaks broaden out and become of finite height. When their shapes are roughly Lorentzian their width in energy can be interpreted as the inverse lifetime, $\tau_k^{-1}$, of the state in question. For comparison with the bands of ordered Ti-Fe in Fig. 1 we have calculated the KKR-CPA Bloch-spectral functions following Faulkner and Stocks.[25] Theses are displayed in Figs. 4, 5, and 6 for, respectively, $\Delta$, $\Lambda$, and $\Sigma$ directions of the bcc Brillouin zone. Evidently there are relatively well-defined bands all through the Brillouin zone. To help with the interpretation of these pictures we have also calculated the band structures for pure Fe and Ti, using the KKR method, on the same lattice as that of the alloy ($a_0=2.975$ Å) and the same potentials as was obtained on the appropriate sites in the self-consistent alloy calculation. The position of these bands at the symmetry points are marked on all three figures.

In all three figures there is a low-energy band starting at the $\Gamma_1$ point. This is an effective $s$ band which is intermediate in energy between the pure Fe and pure Ti $s$ bands. It is customary to refer to such alloy bands as virtual-crystal-like[16] even when they have not been obtained in the virtual-crystal approximation (VCA). The structure higher up in energy constitutes the random-alloy version of the $d$-band complex. Here the formation of the alloy bands is very complicated. The symmetry analysis of the Bloch-spectral function at the $\Gamma$ point shows that

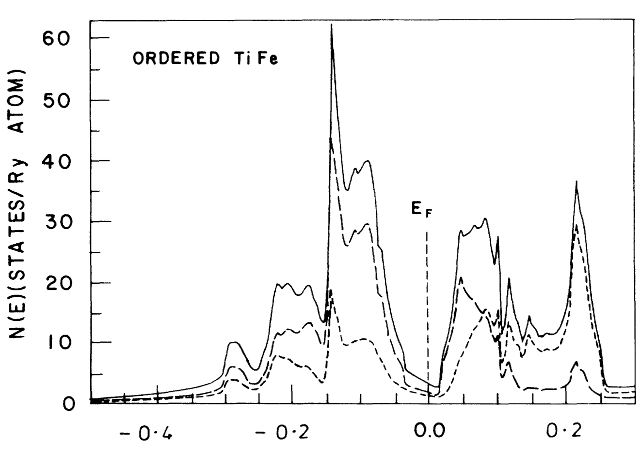

FIG. 2. The density of states of ordered TiFe.

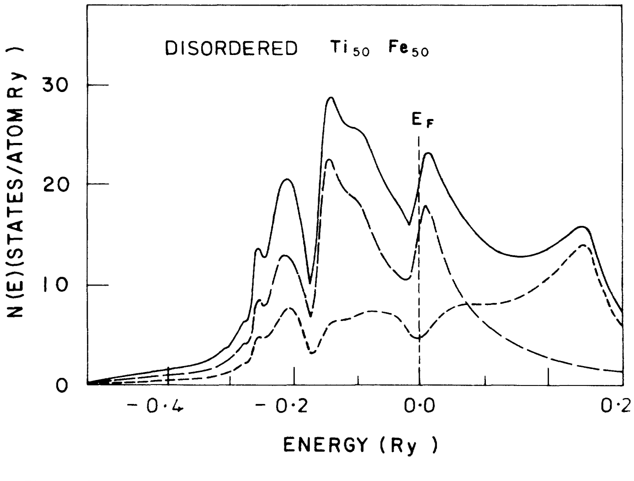

FIG. 3. The density of states of disordered TiFe, solid line; and decomposition into Fe, long-dashed line; and $T_c$, short-dashed line.

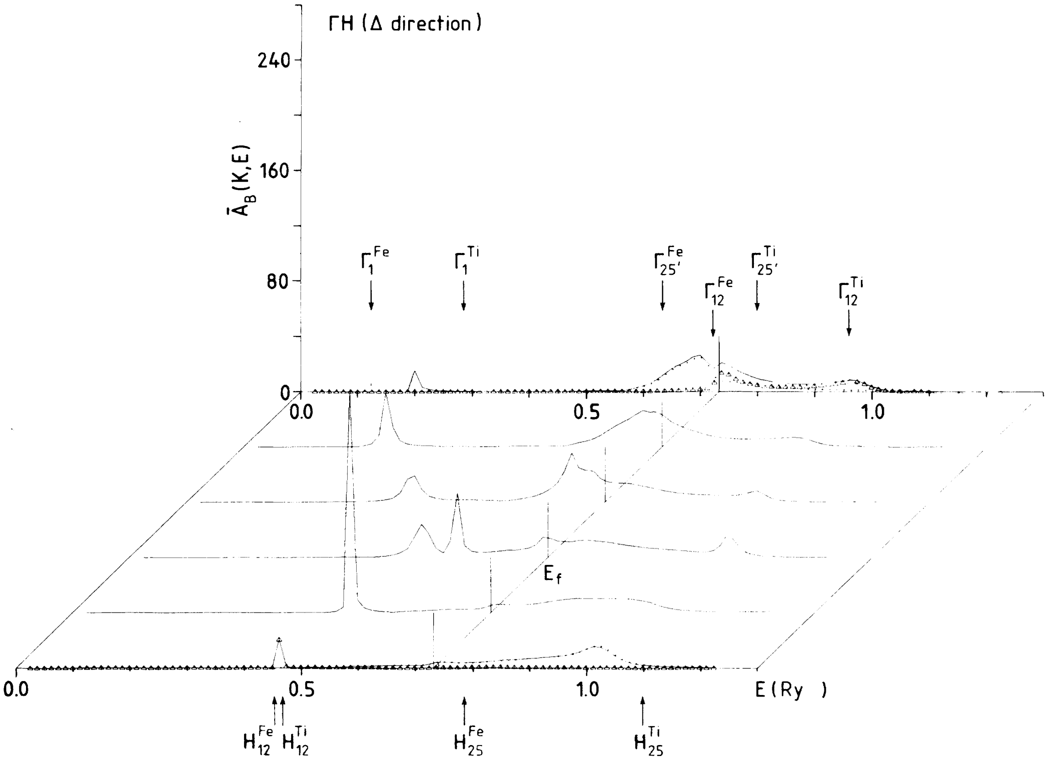

FIG. 4. The Bloch-spectral functions for TiFe along the line Γ$H$ in the bcc Brillouin zone. The Bloch-spectral functions at the Γ and $H$ point are decomposed into $t_{2g}$, open triangles, and $e_g$, dots, contributions.

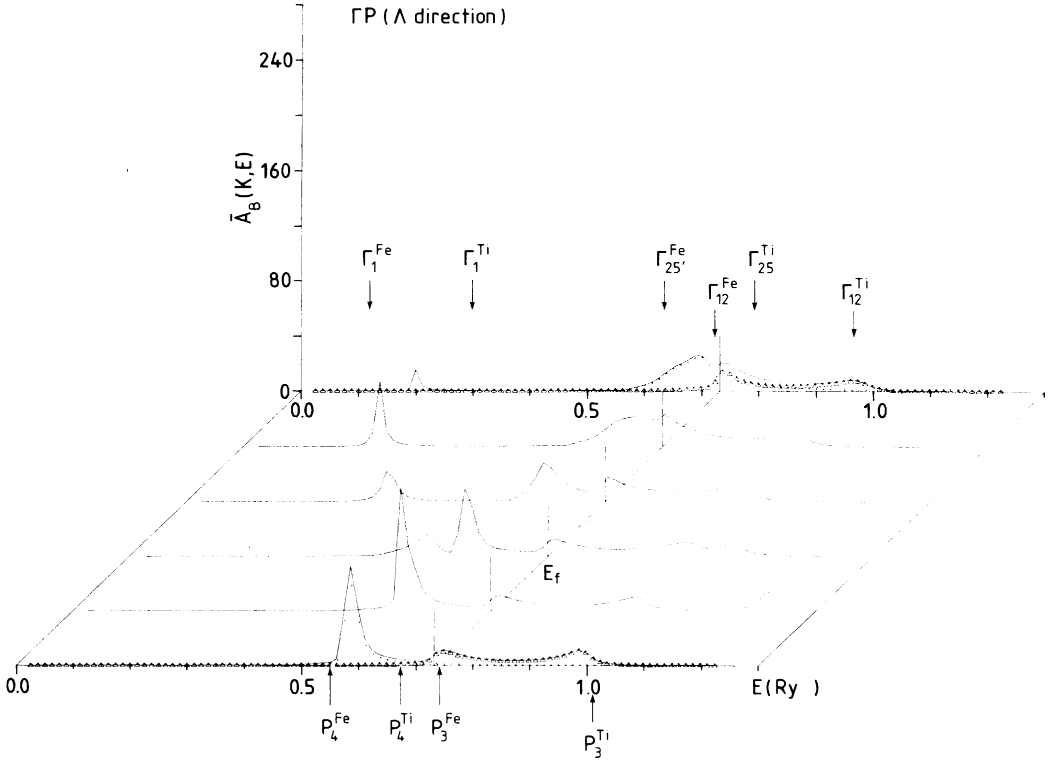

FIG. 5. The Bloch-spectral functions for TiFe along the line Γ$P$ in the bcc Brillouin zone. The Bloch-spectral functions at the Γ and $P$ point are decomposed into $t_{2g}$, open triangles, and $e_g$, dots, contributions.

the *eg* band ($\Gamma_{12}$) is split and each of its peaks can be associated with the pure metal states $\Gamma_{12}^{\mathrm{Ti}}$ and $\Gamma_{12}^{\mathrm{Fe}}$. For the $t_{2g}$ band however we see only one peak at $\varepsilon=0.699$ Ry ($\Gamma_{25}^{\mathrm{Fe}}$) with a shoulder at $\varepsilon=0.780$ Ry ($\Gamma_{25}^{\mathrm{Ti}}$). Going out towards the $H$, $N$, and $P$ points the top part of the $d$ band remains split but the lower the energy the more virtual-crystal-like the bands become. For instance, the Ti $P_4$ and the Fe $P_4$ state appear as a single effective peak at $-0.2$ Ry whereas the Fe $P_3$ and Ti $P_3$ appear separately.

In order to make a direct comparison between ordered and disordered TiFe we have calculated the Bloch-spectral function for disordered TiFe along the $\Delta$, $\Lambda$, and $\Sigma$ directions (Figs. 7, 8, and 9) of the CsCl Brillouin zone. This means that the bands in the Brillouin zone of the bcc structure with one atom per unit cell have to be folded into the Brillouin zone of the CsCl structure with two, but the same, atoms on both sites of the unit cell. We find, for example, the 100 direction ($\Gamma X$) of the CsCl Brillouin to be 100 direction ($\Gamma H$) of the bcc Brillouin zone folded back from the mid point:

$$A_B^{(\Gamma X)_{\mathrm{CsCl}}}=A_B^{(\Gamma H/2)_{\mathrm{bcc}}}+A_B^{(HH/2)_{\mathrm{bcc}}}\ .$$

Using this notation we find for the spectral functions in the $\langle 111\rangle$ and $\langle 110\rangle$ symmetry directions of the CsCl Brillouin zone:

$$A_B^{(\Gamma R)_{\mathrm{CsCl}}}=A_B^{(\Gamma P)_{\mathrm{bcc}}}+A_B^{(HP)_{\mathrm{bcc}}}$$

and

$$A_B^{(\Gamma M)_{\mathrm{CsCl}}}=A_B^{(\Gamma N)_{\mathrm{bcc}}}+A_B^{(HN)_{\mathrm{bcc}}}\ .$$

Of course this folding of the spectral function is completely equivalent to calculating the spectral function for the CsCl structure with two identical atoms per unit cell. We note from the folding-back procedure that all the states on the boundary of the CsCl Brillouin zone, in the case of two identical atoms per unit cell, will at least be double degenerate. For example the bcc $P_4$ and $P_3$ states become $R_{25'}\equiv R_{15}$ and $R_{12}\equiv R_{12'}$ in the CaCl Brillouin zone. In the disordered alloy we find the $P_3$ state split and the $P_4$ state virtual-crystal-like (Fig. 5). Therefore we find in the CsCl Brillouin zone (Fig. 8) two $R_{12}\equiv R_{12'}$ states and one $R_{25'}\equiv R_{15}$ state. This degeneracy, characteristic to the disordered alloy, gets lifted in ordered TiFe. Inspection of Fig. 1 reveals that this degeneracy can be slightly lifted as is the case of the $R_{15}$ and $R_{25'}$ state or by a large amount for the $R_{12}$ and $R_{12'}$. We would say the $R_{15}$ and $R_{25}$ states are of the virtual-crystal-type because it nearly occurs once and the $R_{12}$ and $R_{12'}$ states which are well separated in energy are of the split-band type. The concepts of rigid band and split band used for the disordered alloy in the case of a state occurring once or twice, are therefore also applicable to all the states on the Brillouin-zone boundary of the CsCl structure and we find only small differences in the electronic structure in the $R$ point of ordered and disordered TiFe. Whilst the folding back of the states for a Brillouin-zone boundary point makes all those states at least double degenerate

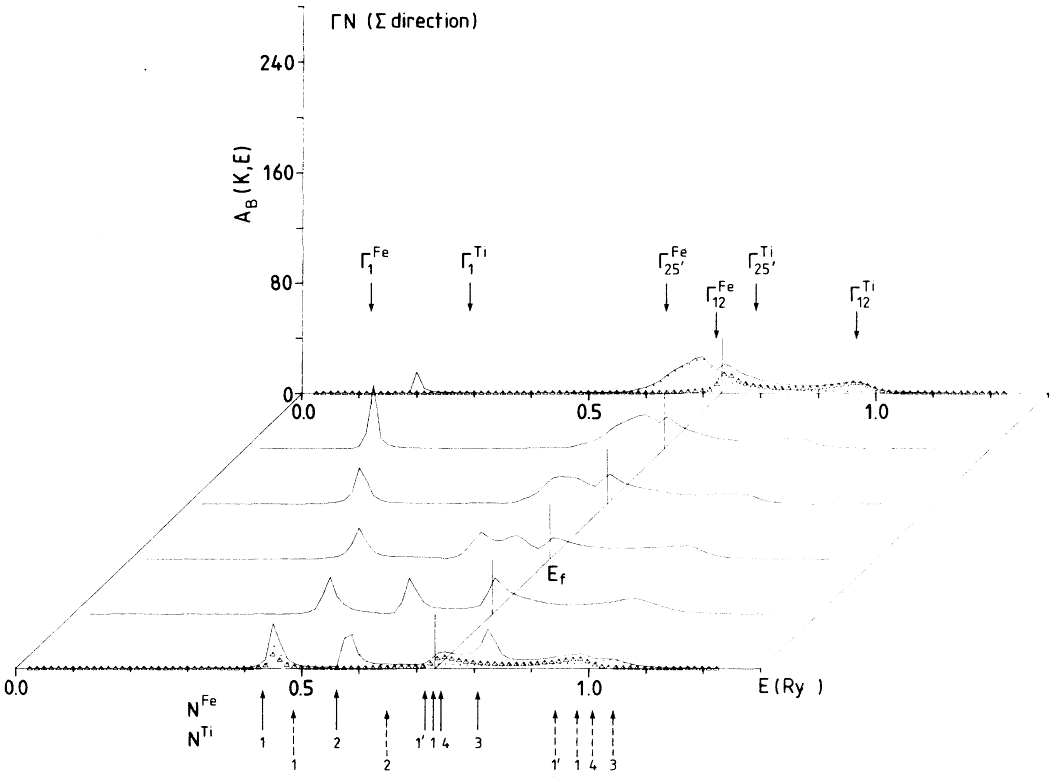

FIG. 6. The Bloch-spectral functions for TiFe along the line $\Gamma N$ in the bcc Brillouin zone. The Bloch-spectral functions at the $\Gamma$ and $N$ point are decomposed into $t_{2g}$, open triangles, and $e_g$, dots, contributions.

$$A_B^{(X)_{\mathrm{CsCl}}} = A_B^{(H/2)_{\mathrm{bcc}}} + A_B^{(H/2)_{\mathrm{bcc}}} ,$$

$$A_B^{(B)_{\mathrm{CsCl}}} = A_B^{(P)_{\mathrm{bcc}}} + A_B^{(P)_{\mathrm{bcc}}} ,$$

$$A_B^{(M)_{\mathrm{CsCl}}} = A_B^{(N)_{\mathrm{bcc}}} + A_B^{(N)_{\mathrm{bcc}}} ,$$

we find for the Brillouin center on the contrary:

$$A_B^{(\Gamma)_{\mathrm{CsCl}}} = A_B^{(\Gamma)_{\mathrm{bcc}}} + A_B^{(H)_{\mathrm{bcc}}} .$$

In the bcc Brillouin zone for the disordered alloy all of the four states: $\Gamma_{12}$, $\Gamma_{25'}$, $H_{12}$, and $H_{5'}$ can be either split or virtual-crystal-like. Therefore we can find in the CsCl Brillouin zone for the disordered alloy from $2\Gamma_{12}$ and $2\Gamma_{25'}$ (virtual-crystal-like) up to $4\Gamma_{12}$ and $4\Gamma_{25'}$ states (extreme split band). For the ordered systems in the CsCl structure only $2\Gamma_{12}$ and $2\Gamma_{25'}$ can occur. In contrast to the disordered alloy, neither split nor rigid band in the sense of a state occurring twice or once can occur at the zone center in the ordered CsCl structure. For TiFe this will lead to small changes in the electronic structure on the Brillouin-zone boundary and big changes in the one-electron spectrum between the ordered and disordered alloy in the Brillouin center.

Compare the disordered (Figs. 7, 8, and 9) and ordered (Fig. 1) electronic structures in Table I. We note that excellent overall agreement in the electronic structure of the ordered and disordered alloy. At the $\Gamma$ point we find the difference in energy between the ordered and disordered $\Gamma_1$ state of 9 mRy. The lower $\Gamma_{25'}$ state has moved up by 25 mRy in the disordered alloy and has also acquired some structure. But the most striking result we find is the upper $\Gamma_{12}$ state at $\varepsilon_{0.830}$ Ry in ordered TiFe splits in the disordered alloy: $\varepsilon_{\Gamma_{12}^{u},1}=0.736$ Ry, $\varepsilon_{\Gamma_{12}^{u},2}=0.973$ Ry. This pushes the upper $\Gamma_{25'}$ up by 40 mRy. This split-band behavior of the upper $\Gamma_{12}$ gives also rise to the following changes in the one-electron states at the $\Gamma$ point: the $\varepsilon_{\Gamma_{12}^{u},1}$ state has a tail which extends to below the Fermi energy whilst the $\varepsilon_{\Gamma_{25}^{l\prime}}$ state has its weight extending above the Fermi energy, leading to a lowering in $E_F$ of 15 mRy. Moreover, we find in the disordered alloy a flat $\Lambda_3$ band at the Fermi energy, contributing to the big change in $n^{\mathrm{dis}}(\varepsilon_F)/n^{\mathrm{or}}(\varepsilon_F)\cong 6$. At the $R$ point on the other hand both the ordered and the disordered alloys have identical alloying behavior: virtual-crystal-like state, the disordered $R_{15}=R_{25'}$ at 0.586 Ry and the ordered $R_{15}$ at 0.591 and Ry and $R_{25'}$ at 0.603 Ry; the ordered split-band states, $R_{12'}$ at 0.747 and $R_{12}$ at 0.989; and the disordered ones, $(R_{12}\equiv R_{12'})^1$ at 0.748 and $(R_{12}\equiv R_{12'})^2$ at 0.986. At the $X$ point we find in ordered TiFe all degeneracies lifted whilst in the disordered alloy only the $X_1$ and $X_{4'}$ states are split. Whilst in the disordered alloy all the states are either rigid band or split band in the sense of the states occurring once or twice, for the ordered compound only the

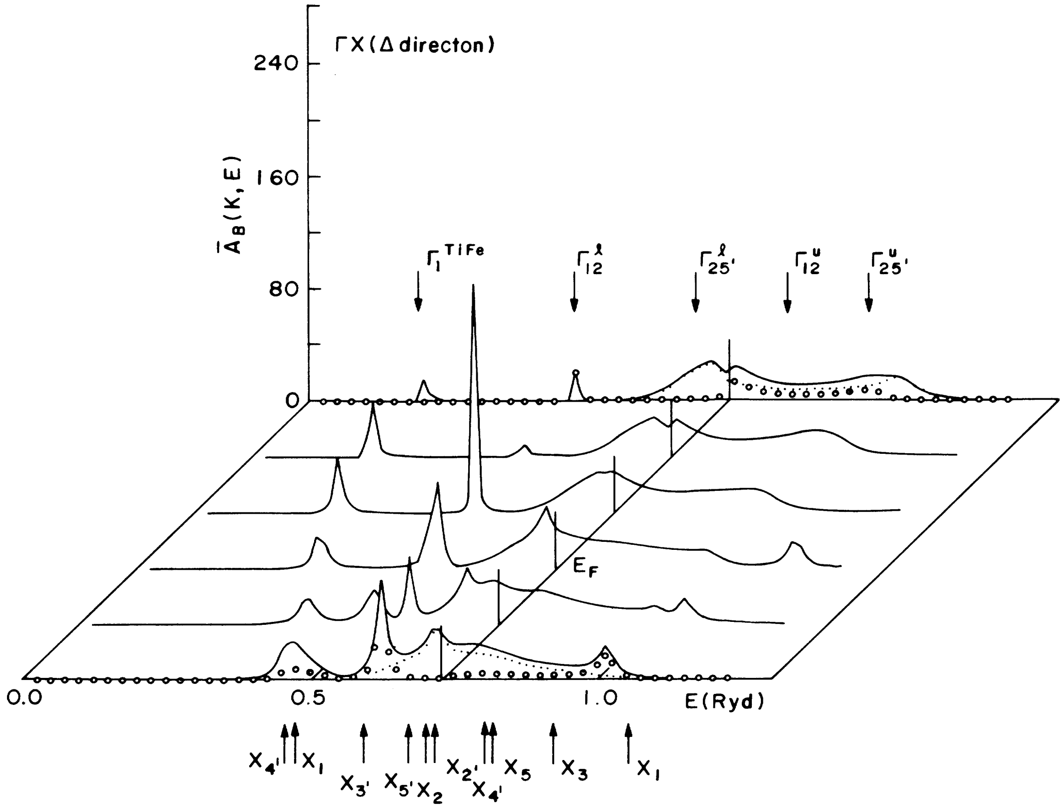

FIG. 7. The Bloch-spectral functions for TiFe along the line $\Gamma X$ in the SC Brillouin zone. The Bloch-spectral functions at the $\Gamma$ and $X$ points are decomposed into $t_{2g}$, open circles, and $e_g$, dots, contributions. The arrows are the ordered TiFe states at the $\Gamma$ and the $X$ point.

states on the Brillouin-zone boundary correspond to this type of rigid-band or split-band behavior. For all the states of the ordered alloy the distribution of their wave-function coefficients over the sites will determine their split-band or rigid-band behavior as reflected in the partial density of states. But note that the split band for the disordered alloy always occurs twice, in the ordered alloy it mostly occurs once. Therefore we can expect to see large changes in the one-electron spectra between the ordered and the disordered alloy in the energy region of the split bands. The one-electron changes seem to be big enough to be seen in angular-resolved photoemission calculations on CuZn (Ref. 26) and experiments on $Cu_3Au$.[27]

Comparing the ordered and the disordered bands the split-band behavior is much more pronounced around the Brillouin zone center in the disordered alloy, but it has less tendency for split-band behavior at and towards the Brillouin-zone boundaries. From the inspection of the Bloch-spectral functions we can see that around $E_F$ the weight of the density of states comes from the Brillouin-zone center and in this density of states the Fe($e_g$) Ti($t_{2g}$) contributions dominate. We note the interesting fact that while the low-energy virtual-crystal-like bands are roughly at the same energy as the Ti-Fe low-energy bonding bands the split $d$ bands within 2 eV or so of $E_F$ are at higher energies than the Ti-Fe bands. As we have suggested earlier this is the energy difference which may be stabilizing the ordered phase. We can now see more clearly that the loss of Ti—Fe bonding in the energy range 0.15 Ry $< E < E_F$ is due to the formation of split Fe and Ti bands in the disordered state. We also confirm that the low-energy states appear to be as bonding in the random alloy as in the ordered state. Plausibly, this is the consequence of the fact that these are virtual-crystal-like effective states with roughly equal amplitudes on each kind of sites. Thus, surprisingly, it is not necessary that all nearest-neighbor pairs be unlike atoms for strong unlike atom bonding in metal.

To the above interpretation of our results we can add one further observation. We calculate the total charge in the Wigner-Seitz polyhedra of equal volume surrounding the Ti and Fe site. For this particular apportioning of space between the two kinds of atoms the charge transfer is measured by the deviation from neutrality in each unit cell. By this definition in the ordered calculation we find a charge transfer from Ti to Fe equivalent to 0.34 electrons. The corresponding figure in the disordered state is 0.27 electrons. This slight reduction in the charge transfer is consistent with the picture of fewer Ti—Fe bonding states.

## IV. CONCLUSIONS

We have investigated the self-consistent electronic structure of the strongly ordering Ti-Fe system both in the ordered and in the disordered phase. From the fairly

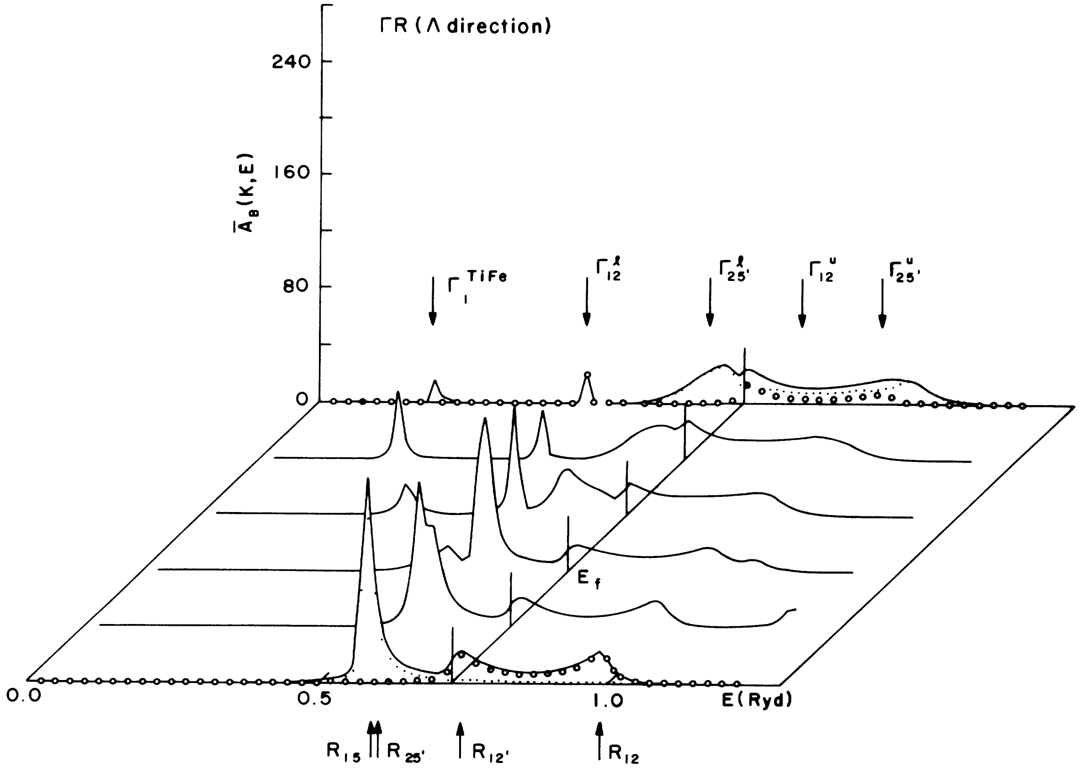

FIG. 8. The Bloch-spectral functions for TiFe along the line Γ$R$ in the SC Brillouin zone. The Bloch-spectral functions at the Γ and $R$ point are decomposed into $t_{2g}$, open circles, and $e_g$, dots, contributions. The arrows are the ordered TiFe states at the Γ and at the $R$ point.

unequivocal shifts in the band energies on ordering we were able to infer the basic features of an electronic mechanism which stabilizes the ordered structure.

Over the past ten years or so a large number of CPA calculations[16,17,18] have shown that a generic electronic structure of random solid solutions consists of bands well defined in energy on the scale of their separation. Moreover, these bands fall into two characteristic classes: effective virtual-crystal bands which are intermediate between the corresponding bands of the pure constituents and split bands which are broadened versions of pure metal bands, one for each constituent. In the former case the amplitude of a state is roughly the same on all sites while the wave functions corresponding to the latter are localized on one of the species. Which of these two behaviors will dominate in a given region of energy and wave vector is determined by the ratio of the separation between the states of the pure constituents to some appropriate local band width. The calculations we have reported here suggest that these two kinds of bands play two distinct roles in ordering.

The virtual-crystal-like bands can bond as well as the corresponding bands of the ordered solid. Hence they are rather neutral as far as the state of order is concerned. This makes it clear that bonding bands in a metal should not be thought of as nearest-neighbor bonds. Moreover, our calculations strongly suggest that the cohesion in the Fe-Ti system comes from the low-lying virtual-crystal bands. Consequently it supports the conventional wisdom that the basic bcc structure of Fe-Ti is due to the half-filled *d* band.[11,15] On the other hand, we have concluded that the state of compositional order is not governed by the above set of bands, but is due to those which can be said to be in the "split-band" regime in the disordered state. This observation is new and complements the real-space arguments of Heine and Samson.[12] From this point of view it is important to stress that the phenomena we are describing in reciprocal space is also quite general. If filled split bands replace bonding bands of lower energy then the ordered state is favored. Presumably if the split bands are lower in energy than the bands of the ordered system, then the composition fluctuations will be of the clustering type and instead of ordering, the system will phase separate. Again it is clear that more than nearest-neighbor bonds are involved. Evidently, whether the right physics is more apparent in the real space or the *k*-space description depends on the particular system at hand. In the case of the Fe-Ti system the latter seems to be more revealing.

Clearly, the above simple general picture can have far-reaching consequences for our understanding of ordering

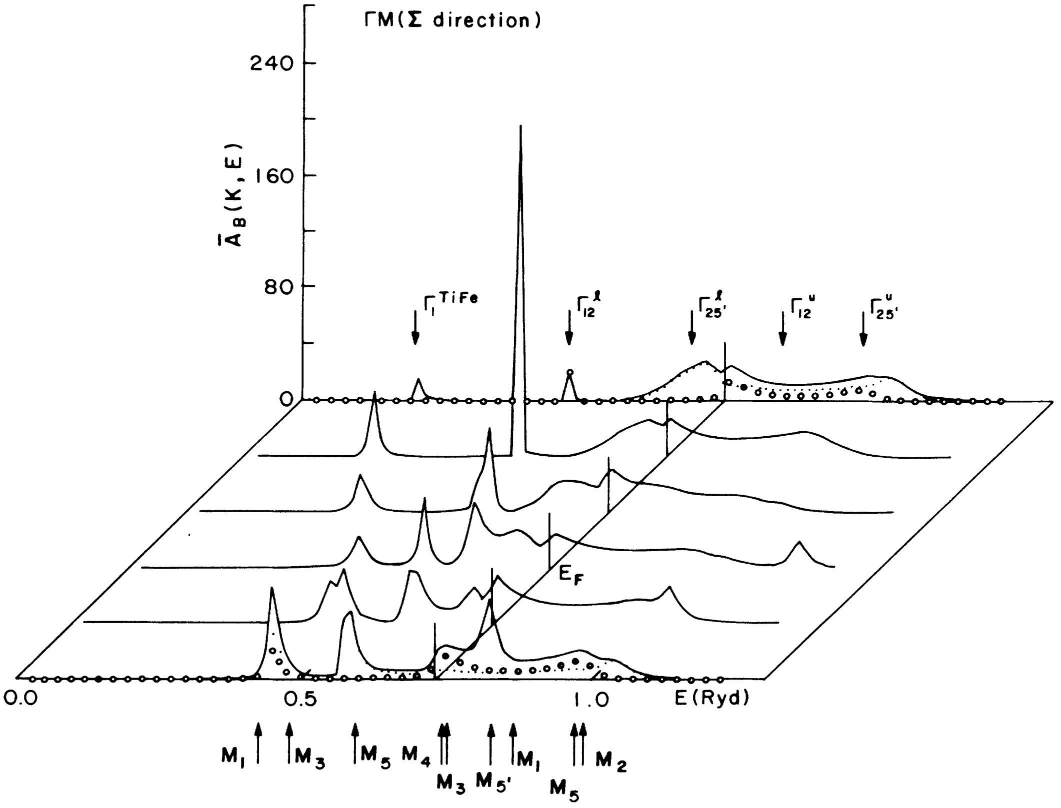

FIG. 9. The Bloch-spectral functions for TiFe along the line $\Gamma M$ in the SC Brillouin zone. The Bloch-spectral functions at the $\Gamma$ and $M$ point are decomposed into $t_{2g}$, open circles, and $e_g$, solid circles, contributions. The arrows are the ordered TiFe states at the $\Gamma$ and at the $M$ point.

and clustering in metallic alloys. Thus experiments which could confirm or reject its premises would be of considerable interest. At the moment the most relevant experimental probe appears to be angle-resolved photoemission spectroscopy (ARPS). As was shown by Allen *et al.*[28] this can follow in detail the bands of disordered solids and that of the pure metals. Evidently the need is to study the ordered alloys as well as at the same time the disordered ones as was recently done.[29]

The relevance of these remarks to the Ti-Fe which does not have naturally occurring disordered phase is that it might be of interest to make randomized Ti-Fe by irradiation with neutrons or electrons. Such a metastable phase might still retain the bcc phase while losing the compositional order and hence the bands we have identified as being the electronic barrier to disorder could be studied by ARPS. One might object that there are other ordering systems to investigate where the ordered and disordered phases are more accessible. However, there is merit in studying such an extreme case as Ti-Fe because here the main features of the ordering mechanism are so clearly present.

## ACKNOWLEDGMENTS

One of us (E.Z.S) would like to thank the H.H. Wills Laboratory and the Daresbury Laboratory for their hospitality under the CCP-9 program. He also thanks Professor E. Galvão da Silva for interesting him in this problem. A travel grant from Conselho Nacional de Desenvolvimento Científico e Tecnológico (CNPq) and the Royal Society is gratefully acknowledged.

---

[1] E. Wigner and F. Seitz, in *Solid State Physics*, edited by F. Seitz, D. Turnbull, and H. Ehrenreich (Academic, New York, 1955), Vol. 1, p. 97.

[2] V. L. Moruzzi, J. F. Janak, and A. R. Williams, *Calculated Electronic Properties of Solids* (Pergamon, New York, 1978).

[3] W. Kohn and P. Vashishta, in *Theory of the Inhomogeneous Electron Gas*, edited by S. Lundqvist and N. March, (Plenum, New York, 1983).

[4] H. J. F. Jansen and A. J. Freeman, Phys. Rev. B **30**, 561 (1984).

[5] G. M. Stocks and H. Winter, in *Electronic Structure of Complex Systems*, Vol. 113 of *NATO Advanced Study Institute, Series B: Physics*, edited by P. Phariseau and W. M. Temmerman (Plenum, New York, 1984).

[6] D. de Fontaine, in *Solid State Physics*, edited by F Seitz, D. Turnbull, and H. Ehrenreich (Academic, New York, 1979), Vol. 34, p. 73.

[7] W. Hume-Rothery, *The Structure of Metals and Alloys* (Institute of Metals, 1954).

[8] H. Winter and G. M. Stocks, Phys. Rev. B **27**, 882 (1983).

[9] H. Winter, P. J. Durham, W. M. Temmerman, and G. M. Stocks (unpublished).

[10] W. B. Pearson, in *Developments in the Structural Chemistry of Alloy Phases*, edited by B. C. Giessen, (Plenum, New York, 1969).

[11] D. G. Pettifor, in *Physical Metallurgy*, edited by R. W. Cahn and P. Haasen (North-Holland, Amsterdam, 1983), Ch. 3.

[12] V. Heine and J. H. Samson, J. Phys. F **13**, 2155 (1983).

[13] B. L. Gyorffy and G. M. Stocks, Phys. Rev. Lett. **50**, 374 (1983).

[14] N. Mott, Adv. Phys. **13**, 325 (1964).

[15] J. Friedel, in *Metallic Solid Solutions: A Symposium on their Electronic and Atomic Structure*, edited by J. Friedel and A. Guinier (Benjamin, New York, 1963).

[16] B. L. Gyorffy and G. M. Stocks, in *Electrons in Disordered Metals and at Metallic Surfaces*, Vol. 24 of *NATO Advanced Study Institute, Series B: Physics*, edited by P. Phariseau, B. L. Gyorffy, and L. Scheire, (Plenum, New York, 1979).

[17] J. S. Faulkner, Prog. Mat. Sci. **27**, 3 (1982).

[18] H. Ehrenreich and L. M. Schwartz, in *Solid State Physics*, edited by F. Seitz, D. Turnbull, and H. Ehrenreich (Academic, New York, 1976), Vol. 31, p. 150.

[19] O. K. Andersen, Phys. Rev. B **12**, 3060 (1975).

[20] H. L. Skriver, *The LMTO Method*, Vol. 41 of *Springer Series in the Solid State Sciences* (Springer, Berlin, 1984).

[21] G. M. Stocks, W. M. Temmerman, and B. L. Gyorffy, in *Electrons in Disordered Metals and Metallic Surfaces*, Ref. 16.

[22] J. Yamashida and S. Asano, Prog. Theor. Phys. **48**, 2119 (1972).

[23] D. A. Papaconstantopoulos, Phys. Rev. B **11**, 4801 (1975).

[24] N. G. Kamm, Phys. Rev. B **12**, 3013 (1975).

[25] J. S. Faulkner and G. M. Stocks, Phys. Rev. B **21**, 3222 (1980).

[26] P. J. Durham, W. M. Temmerman, C. G. Larsson, and P. O. Nilsson, Vacuum **33**, 771 (1983).

[27] R. G. Jordan, G. S. Sohal, B. L. Gyorffy, P. J. Durham, W. M. Temmerman, and P. Weinberger, J. Phys. F **15**, L135 (1985).

[28] N. K. Allen, P. J. Durham, B. L. Gyorffy, and R. G. Jordan, J. Phys. F **13**, 223 (1983).

[29] P. J. Durham, in *Electronic Structure of Complex Systems*, Vol. 113 of *NATO Advanced Study Institute, Series B: Physics*, Ref. 5.